



ISSN NO. 2320-5407

Journal homepage: <http://www.journalijar.com>

INTERNATIONAL JOURNAL
OF ADVANCED RESEARCH

RESEARCH ARTICLE

Attenuation characteristics of seismic body waves for the crust of Lower Siang region of Arunachal Himalaya

Rohtash Kumar, S. C. Gupta and Arjun Kumar

Department of Earthquake Engineering Indian Institute of Technology, Roorkee-247667 Uttarakhand (INDIA).

Manuscript Info

Manuscript History:

Received: 15 April 2014
Final Accepted: 22 May 2014
Published Online: June 2014

Key words:

attenuation, Q_α , Q_β , Lower Siang, Arunachal Himalaya.

Corresponding Author

Rohtash Kumar

Abstract

The seismic wave attenuation characteristics for the crust of Lower Siang region of Arunachal Himalaya have been investigated using a data set of 104 local earthquakes. The frequency dependence relationships of quality factors for P-wave (Q_α) and S wave (Q_β) have been estimated by using extended coda wave normalization method in the frequency range 1.5 Hz to 24 Hz. The average variation in the estimated value of Q_α and Q_β are from 49 at 1.5 Hz to 1421 at 24 Hz and 118 at 1.5 Hz to 2335 at 24 Hz respectively. The frequency dependent relations for P and S-waves are $(25 \pm 3)f^{(1.24 \pm 0.04)}$ and $(62 \pm 9)f^{(1.13 \pm 0.04)}$ respectively. The value Q_α and Q_β obtained in the present study are comparable with the other seismically active regions of the world as well as of India. The Q_β/Q_α ratio is found greater than unity over the entire range of the frequencies which indicates the importance of contribution of the scattering attenuation to the body waves in the study region. Also $Q_\beta/Q_\alpha > 1$ indicates that the crust is highly heterogeneous in this region of Himalaya. The estimated S wave attenuation is compared with the coda wave attenuation (Q_c) obtained by Kumar et al., (2014) for this region. The estimated Q_β is found less than Q_c over entire frequency range which supports the Zeng et al. (1991) model that explained that the Q_c contains the combined effect of scattering and intrinsic attenuation. The obtained attenuation relations in the present study will be useful for simulation of strong ground motion and for estimation earthquake source parameters which have been further required for seismic hazard assessments in this region.

Copy Right, IJAR, 2014.. All rights reserved.

Introduction

The basic physical mechanisms which are responsible for the loss of energy of propagating seismic waves are intrinsic absorption from inelasticity of rocks and scattering due to heterogeneities present in the path of seismic waves. The seismic energy is converted into the heat by intrinsic absorption and redistributed due to the internal heterogeneous medium through which the seismic wave passes. The higher frequency component of seismic waves attenuates more rapidly than the low frequency components resulting in resolution loss in seismograms. Therefore, the attenuation of seismic waves in the lithosphere is an important property for studying the regional earth structure in relation to seismicity (Mandal et al., 2004). On the earthquake ground motion the effect of traveled path is mainly due to the attenuation of propagation seismic waves. The efficiency of seismic energy propagation through a medium is commonly expressed by the inverse of dimensionless quantity called quality factor Q (Knopoff, 1964).

$$Q^{-1} = \Delta E / 2\pi E,$$

Where E is the total energy available in a harmonic wave and ΔE is the energy lost in one cycle. An essential property of the earth reflecting its composition and thermal state is described by the attenuation parameter. Wave attenuation is one of the most important parameter which is directly related to medium properties of study region and essential for many studies such as exact determination of earthquake source parameters (Abercrombie,

1997), prediction of earthquake ground motions (Chopra et al., 2010), monitoring nuclear explosions (Mayeda et al., 2003) and the assessment of seismic hazards in a region (Anderson et al., 1996, Gupta et al., 1998). Also, attenuation parameter Q^{-1} is essential for understanding the physical mechanism of seismic wave attenuation in relation to the composition and physical condition of the earth's interior (Liu et al., 1976; Sato, 1992). As seismic wave attenuation is effected by the tectonic activity so in tectonically active region it is also used to investigate tectonic properties and structure in the region (Aki, 1980). The seismic wave attenuation can be estimated using P-wave (Q_α), S-wave (Q_β) and/or coda waves (Q_c) observed on a seismogram which is recorded at local or regional distances.

In a region, seismic wave attenuation can be estimated by a number of techniques and different parts of the seismogram (Aki, 1969; Aki and Chouet, 1975; Hermann, 1980; Mitchell, 1995). Aki (1980) proposed the coda normalization method to estimate the frequency-dependent relation for Q_β . Yoshimoto et al. (1993) extended this method for simultaneous measurement of Q_α and Q_β which is successfully applied in the various regions of India and world, e.g., Koyana, India (Sharma et al. 2007); Bhuj, India (Padhy, 2009); Kanto, Japan (Yoshimoto et al. 1993); Western Nagano, Japan (Yoshimoto et al. 1998); South-Eastern Korea (Chung and Sato, 2001); central South Korea (Kim et al., 2004); East-Central Iran (Mahood et al., 2009) and Cairo metropolitan area (Abdel-Fattah, 2009). The attenuation characteristics vary from one region to another. It has been observed that in the seismically active regions, the Q factor is low as compared to stable regions (Sekiguchi, 1991; Fedotov and Boldyrev, 1969; Masuda, 1988; Sato and Fehler, 1998). As per the requirement of engineering seismology the attenuation characteristics of S waves have been studied more intensively than P wave. In the same region, the Q_α , and Q_β are different another (Rautian et al., 1978). A very few studies have been done for the simultaneous estimation of frequency dependent Q_α and Q_β (Hough and Anderson, 1988; Masuda, 1988; Campillo and Planet, 1991; Yoshimoto et al., 1993; Sharma et al., 2007, 2008, 2009). The attenuation of high frequency P and S waves in the earth has been summarized by Der (1998).

In the present study attempt has been made to understand the seismic body wave's attenuation characteristics in lower Siang region of Arunachal Himalaya. The region is one among the highest seismically active regions and undergone many deformations and reactivation of some of the faults, thrusts etc, and monitoring of seismic activity of this region by seismological and strong motion network is of importance (Kumar et al., 2006, 2012, 2013a, b). For this purpose Q_α and Q_β are estimated using extended coda normalization method (Yoshimoto et al., 1993). Waveform data of 104 local earthquakes recorded by local seismological network deployed in lower Siang region of Arunachal Himalaya have been used for the analysis.

Geology and Seismotectonic of the Region

The Lower Siang region (Fig. 2) belongs to major antiformal tectonic unit called Eastern Syntaxis, which show a bend in their regional strike from ENE–WSW to NW–SE. The regional stratigraphy of this zone has been established by various researchers (Singh, 1993; Kumar, 1997; GSI, 2006). The Eastern Syntaxis is built up of Proterozoic to Cenozoic rocks arranged in distinct litho-tectonic belts. The Eastern Syntaxis is a belt where two distinct tectonic domains with ENE-WSW trend in the west and NW-SE trend in the east are juxtaposed (Singh, 1996). The Eastern Syntaxis is composed of three major thrust sheets, namely Siang, Siyom and Rikor in descending tectonic order. A complex Para autochthonous zone is exposed in the central part which contains the Abor Volcanic, the Yingkiang Formation and the Dalbung Formation. Rocks exposed in the Eastern Syntaxial region belong to three major units of Himalaya; the Sub-Himalaya (Siwaliks), the Lesser Himalaya (including the Gondwana Group) and the Higher Himalaya (Gansser, 1964). In addition, central part of the syntaxial structure is occupied by a sequence of sedimentary rocks of Eocene age, associated with basic volcanic rocks (Singh, 1993).

From the tectonic point of view, Arunachal Pradesh is unique and is much different than the other parts of Himalaya. It is situated at the junction of three plates; Indian plate, Indo-Burmesen plate and Eurasian plate. The most important elements of Himalayan domain in this region are Tsangpo Suture, Main Central Thrust (MCT), Main Boundary Thrust (MBT) and Main Frontal Thrust (MFT) (Narula et al., 2000). The Lohit Thrust separating the moderately metamorphosed sequence from Granitoid massif of Tuting Group and Mishmi Thrust is also an important structural element of the area. The Bame Fault bears evidences on right lateral sense of movement. Rejuvenation of a conjugate set of faults encompassing Po Chu Fault and one parallel to Bame Fault, during historical past, has been interpreted. There are several sets of neotectonic faults in the Brahmaputra Basin, at the south of Arunachal Himalaya. Of these faults, those trending NE-SW and E-W are the most important (CISMHE, 2011, Kumar, 2011).

The region is, seismologically, one of the most active zone of Himalayan terrains. In the Seismotectonic architecture of the Arunachal Himalaya the main river Tsangpo, follows a Suture zone in Tibet. This river, named Siang in Arunachal Pradesh, is controlled by the axis of Siang Antiform. As per seismic zoning map of India as

incorporated in Indian Standard, (Criteria for Earthquake Resistant Design of Structure IS 1893 (part-I), 2002, 2014: General provision and Buildings), the study area lies in the seismic zone V. The zone V is broadly associated with a seismic intensity of IX or above on modified Mercalli scales (M.M. Scale). The earthquake activity in this region is due to the Indian plate diving beneath the Eurasian plate in the north and subduction below the Burmese plate in the east. Earthquakes here are generally shallow (depth < 40Km) but in the Naga Hills some intermediate focus events have also been occurred (CISMHE, 2011).

Methodology

Aki (1980) proposed the coda normalization method based on the empirical observation to derive frequency dependent attenuation relationship for shear waves (Q_β). Yoshimoto et al. (1993) extended this method for simultaneous measurements both body waves (Q_α and Q_β). For the local earthquakes recorded at distances less than 100 km, the spectral amplitude of the coda at lapse times greater than twice the S wave travel time is proportional to the source spectral amplitude of the S waves (Yoshimoto et al., 1993; Kim et al., 2004). The normalization of S wave spectra to coda removes the effects of source, site and the recording instrument. The Q is estimated under the assumption that P- to S-wave radiations have the same spectral ratio within some magnitude range within narrow frequency range (Yoshimoto et al., 1993). Even if the spectral shapes of P and S waves are different, the assumption holds good (Molnar et al., 1973; Rautian et al., 1978; Sharma et al., 2009). The method is based on the following proportionality between the coda spectral amplitude $A_c(f, t_c)$, the source spectral amplitude of S waves $S_s(f)$ and the source spectral amplitude of P waves $S_p(f)$:

$$A_c(f, t_c) \propto S_p(f) \propto S_s(f) \quad (1)$$

Where $S_p(f)$ is the source spectral amplitude of P waves, $S_s(f)$ is the source spectral amplitude of S waves, f is the frequency in Hz and t_c is the reference lapse time measured from the source origin time.

The Q_α and Q_β can be calculated based on the above proportionality with the analysis of earthquakes of various hypocentral distances.

$$\ln \frac{A_p(f,r)}{A_c(f,t_c)} = -\frac{\pi f}{Q_\alpha V_p} r + \text{cont}(f) \quad (2)$$

$$\ln \frac{A_s(f,r)}{A_c(f,t_c)} = -\frac{\pi f}{Q_\beta V_s} r + \text{cont}(f) \quad (3)$$

Where $A_p(f, r)$ and $A_s(f, r)$ represents the amplitude spectra of the direct P and S waves at the hypocentral distance r (km) respectively. V_p is the P-wave velocity and V_s is the S-wave velocity. The vertical (Z) components of seismograms and horizontal components (N-S) are analyzed for the estimation of Q_α and Q_β respectively. The Butterworth band pass filter has been used for filtering the data at seven different central frequencies (Table 1). The Fig.3 represents the seismogram recorded at LED. The spectral amplitude of the direct P and S waves are measured using 2.56 sec time window. The spectral amplitude of the Coda $A_c(f, t_c)$ is calculated using a lapse time window of 2.56 sec and the lapse time for the analyzed portion of the coda wave is taken as twice the travel time of S-wave (Aki and Chouet, 1975; Rautian and Khalturin, 1978). The geometrical spreading is r^{-1} and $\frac{1}{\sqrt{r h_{\text{moh}}}}$ for the epicentral distance of $r \leq h_{\text{moh}}$ and $r \geq h_{\text{moh}}$, respectively (Chandni et. al., 2012) where h_{moh} is twice the Moho depth (Herrmann and Kijko, 1983; Mahood et al., 2009). In the study region the Moho depth is 46 km (Khattri, 1983) so h_{moh} approximately can be taken as 90km. the hypocenter of the earthquakes considered for the analysis is less than 90 km. Therefore inverse power law of hypocentral distance r^{-1} has been considered for geometrical spreading.

The values of Q_α and Q_β are obtained from the slope of best fitted line derived by fitting linear regression line after applying the least square method. The slope of best fitted line can be obtained by using equation (2) and (3):

$$Q_\alpha = -\frac{\pi f}{\text{Slope} \times V_p} \quad \text{for P-wave} \quad (4)$$

$$Q_\beta = -\frac{\pi f}{\text{Slope} \times V_s} \quad \text{for S-wave} \quad (5)$$

Result and discussion

For Lower Siang region of Arunachal Himalaya the estimated values of Q_α and Q_β at various frequencies shows increase with the increasing frequency. The average values of Q_α vary from 49 at 1.5 Hz to 1421 at 24 Hz, the average values of Q_β vary from 118 at 1.5 Hz to 2335 at 24Hz (Fig. 4). The frequency dependence is comparable with the other seismically active regions of India and world such as Kanto, Japan (YOSHIMOTO et al., 1993), Garda, Italy (CASTRO et al., 2008), South, Eastern Korea (CHUNG and SATO, 2001), Northern Italy (Console & Rovelli, 1981), Central Italy (Castro et al., 2002), South Central Alaska (Dutta et al., 2004), Central South Korea (Kim et al., 2004), Kuchchh region (Chopra et. al., 2008), Chamoli region (Sharma et al., 2009), NE Himalaya (Padhy and Subhadra, 2010), NW Himalaya (Imtiyaz et al., 2012), Koyna region, Gujrat (Sharma, 2009), Mainland

region, Gujarat (Chopra et al., 2010), Saurashtra region, Gujarat (Chopra et al., 2010), Marche, Italy (Castro, 1999), Central South Korea (Kim et al., 2004) and France (Campillo and Planet, 1991). For each station the power law $Q=Q_0f^n$ (where Q_0 is the Q value at 1 Hz and n is the frequency dependence factor) has been fitted to estimate the frequency dependence of Q (Table 3). The average power spectral relation for the Lower Siang region of Arunachal Himalaya region is $(25\pm 3)f^{(1.24\pm 0.04)}$ for P-wave and is $(62\pm 9)f^{(1.13\pm 0.04)}$ for S-wave. It has been observed that the value of Q_α and Q_β in the stable regions is low as compared to that of seismically active regions. The value obtained in the present study is comparable with the other studies in other parts of Himalaya. Also it has been observed that P wave attenuates more rapidly than the S waves ($Q_\beta/Q_\alpha > 1$). Also, in many other regions of the world with high degree of lateral heterogeneities the $Q_\beta/Q_\alpha > 1$ is observed (Bianco et al., 1999; Sato and Fehler, 1998). The geology of the Lower Siang Region of Arunachal Himalaya helps in understanding the heterogeneities in the region. It comprises of alluvium of quaternary period, sedimentary and Dark green to grey amygdaloidal mafic volcanic of Miocene period, sedimentary of Permian period and metamorphic rocks of proterozoic eon. The Sediments of the active channels, Boulders, Cobbles, Pebbles with Sand (Holocene); Boulders, cobbles, gravel, silt, clay (Pleistocene); Soft grey sandstones, silt, clay and semi-consolidated gravel-boulder beds; Miri Formation Conglomerate (Lower Permian); Quartzite and shale/slate with conglomerate lenses of Nikte Quartzite (Lower to Middle Palaeozoic) and other igneous intrusions make the regions highly heterogeneous. Hence this part of Himalaya is highly heterogeneous and highly seismically active region than the other parts of the Himalaya.

The Q -values obtained in the present study are compared with the Coda Q -value (Q_c) obtained by Kumar et al. (2014, under review) using single scattering method (Aki, 1980). It has been found that Q_β is less than Q_c (Fig.5) which supports the Zeng et al. (1991) model. He explained that Q_c is more than Q_β because Q_c contains the combined effects of intrinsic and scattering attenuation. Aki (1980) observed Q_c is approximately equal to Q_β because coda waves are backscattered S-waves. Wennerberg (1993) explained this variation of Q_c and Q_β caused by the relative weakness in scattering attenuation.

Attenuation Mechanisms

Seismic waves get attenuated mainly due to intrinsic and scattering mechanism. The internal particle friction is responsible for intrinsic attenuation that converts seismic energy to heat energy. Whereas the scattering is attributed to the heterogeneities present in the medium (Sato and Fehler, 1998). Geologically the heterogeneities caused by different processes such as faulting, folding, large-scale crustal movements associated with plate tectonic. It is more complicated to discuss the intrinsic part further as in the present study; there is no evidence of the controlling factors of the intrinsic attenuation. However, Kumar et al. (2014, under review) analyze some local earthquake data using the multiple lapse time windows (MLTW) and shows that the dominated mechanism of attenuation in the Lower Siang region is scattering attenuation which is also supported by the geological and tectonic features of the area. So the presence of many faults and complex geological formation reveals their contribution for scattering of seismic wave attenuation as an important factor. It is expected that in the highly heterogeneous region where the scattering is more prominent, the Q_β/Q_α ratio is high (Padhy, 2009). The study of Hough and Anderson (1988) also pointed that Q_β/Q_α is greater than one for heterogeneous regions causing scattering of seismic wave energy. Hence, observed high value of Q_β/Q_α in the study reveals the presence of shallow heterogeneities in crust of study area.

Comparison of Q_α and Q_β with global observations

The Q_α and Q_β observed in the present study are compared with the other studies carried for the different regions of world and India (Fig. 6a, b, c, d). The frequency dependent relationships for Q_α and Q_β are comparable with the other seismically active regions of the world and India such as Kuchchh region (Chopra et al., 2008), NE Himalaya (Padhy and Subhadra, 2010), NW Himalaya (Imtiyaz et al., 2012), Kanto, Japan (YOSHIMOTO et al., 1993), Kumaun Himalaya (Singh et al., 2012), Marche, Italy (Castro, 1999), Central Italy (Castro et al., 2002), Garda, Italy (Castro et al., 2008) and Koyna region, Gujarat (Sharma, 2009), low Q values are observed. However, for comparatively stable regions such as Central South Korea (KIM et al., 2004) and Baltic Shield (Kvamme and Havskov, 1989), their Q value is high. Also the average Q_β/Q_α ratio at 1 Hz is compared with the other regions of the world (Fig. 7). The results obtained in this study for lower Siang region shows $Q_\beta > Q_\alpha$. The dash line $Q_\beta = 2.25Q_\alpha$ (i.e. $Q_\beta/Q_\alpha = 4/9$) is theoretically derived. Sekiguchi (1991) investigated the 3-D wave attenuation in Kanto-Tokai area using the spectral ratio method. He assumed frequency independent Q_α and also fixed the Q_β/Q_α equal to 4/9. The theoretically derived Q_β/Q_α ratio is approximately accounts the attenuation of low frequency seismic waves having frequency less than 0.1 Hz (Anderson et al., 1965; Yoshimoto et al., 1993). The laboratory measurements done by Toksoz et al. (1978) shows that in water saturated rocks the Q_β/Q_α ratio is less than unity while in dry rocks it is greater than unity. Yoshimoto et al. (1993) found that this assumed ratio is not applicable for higher frequencies and observed that Q_β/Q_α is greater than unity for Kanto area, Japan for frequencies greater than 1 Hz. This observed ratio is approximately close to V_α/V_β ratio, which is also obtained by Rautian et al. (1978) for crust of Garm region.

Yoshimoto et al. (1998) explained that Q_β/Q_α is greater than unity for frequency range about 1–30 Hz. The observed Q_β/Q_α for Oaxaca subduction zone in Mexico is 2.54 for the frequency range 1.5-24Hz. Chung and Sato (2001), analyzing the earthquake data of Yangsan fault region of south-eastern South Korea found that in the frequency range 1.5–24 Hz, the Q_β/Q_α ratio approximately equal to the 2.25. For Koyna region (India), Sharma et al. (2007) obtained the Q_β/Q_α greater than unity for frequencies 1.5–18 Hz. For Kanto region (Japan) the observed $Q_\beta/Q_\alpha \geq 1$ in frequency range 1–10 Hz. Padhy (2009) for Bhuj region (India) found that the Q_β/Q_α is greater than unity for frequency range of 1–24 Hz. Recently Singh et al (2012) reports the Q_β/Q_α for Kumaon Himalaya in the frequency range 1.5-12 Hz. Hence the present study obtained Q_β/Q_α ratio is quite agreed with the other worldwide reported values.

Table 1: Site characteristics and epicentral locations of the recording stations

| Sl. No. | Name of Station | Station Code | Lat. (°N) | Long. (°E) | Elev. (meters) | Type of Soil/Rock |
|---------|-----------------|--------------|-----------|------------|----------------|------------------------------|
| 1. | Adi-Pasi | ADI | 28.36° | 95.26° | 997 | Reddish Sandstone with Shale |
| 2. | Ahali-Suru | AHO | 28.24° | 95.54° | 571 | Quartzite |
| 3. | Ayeng | AYE | 28.15° | 95.36° | 272 | Boulder Bed |
| 4. | Ledum | LED | 27.96° | 95.13° | 385 | Boulder bed |
| 5. | Rotung | ROT | 28.14° | 95.16° | 410 | Quartzite |
| 6. | Yeksi | YEK | 28.24° | 94.98° | 401 | Conglomerate |

Table 2: Central frequency components of bandpass filter with low and high cut-off frequencies

| Low cut-off (Hz) | Central frequency (Hz) | High cut-off (Hz) |
|------------------|------------------------|-------------------|
| 1.00 | 1.50 | 2.00 |
| 2.00 | 3.00 | 4.00 |
| 4.00 | 6.00 | 8.00 |
| 6.00 | 8.00 | 12.00 |
| 8.00 | 12.00 | 16.00 |
| 12.00 | 18.00 | 24.00 |
| 16.00 | 24.00 | 32.00 |

Table 3: Average values of Q_α and Q_β along with their standard deviations at different central frequencies at five stations.

| Frequency (Hz) | ADI (Q_α) | (Q_β) | AHO (Q_α) | (Q_β) | AYE (Q_α) | (Q_β) | LED (Q_α) | (Q_β) | ROT (Q_α) | (Q_β) |
|----------------|--------------------|---------------|--------------------|---------------|--------------------|---------------|--------------------|---------------|--------------------|---------------|
| 1.5 | 46±4 | 101±5 | 56±4 | 130±6 | 33±4 | 109±5 | 71±6 | 123±7 | 42±4 | 128±7 |
| 3.0 | 91±4 | 135±3 | 92±3 | 132±4 | 75±3 | 199±4 | 99±3 | 169±3 | 106±3 | 180±4 |
| 6.0 | 253±6 | 346±5 | 200±4 | 404±5 | 206±4 | 416±4 | 212±3 | 436±4 | 222±3 | 490±5 |
| 9.0 | 412±6 | 606±4 | 360±4 | 654±5 | 383±4 | 722±4 | 435±5 | 955±6 | 374±3 | 698±4 |
| 12.0 | 580±6 | 808±3 | 488±4 | 955±4 | 590±5 | 1097±5 | 714±6 | 1939±8 | 585±4 | 1007±4 |
| 18.0 | 1025±7 | 1240±3 | 743±4 | 1471±4 | 1070±6 | 1867±6 | 1335±7 | 2725±8 | 937±4 | 1713±4 |
| 24.0 | 1528±9 | 1654±3 | 984±4 | 1996±5 | 1273±5 | 2194±5 | 1999±9 | 3574±8 | 1325±5 | 2261±4 |

Table 4: Frequency dependent relationships for five stations.

| Station code | Relation for p waves | Relation for s waves |
|--------------|--|---|
| ADI | $Q_\alpha = (19 \pm 2)f^{(1.31 \pm 0.03)}$ | $Q_\beta = (55 \pm 4)f^{(1.07 \pm 0.02)}$ |
| AHO | $Q_\alpha = (34 \pm 3)f^{(1.06 \pm 0.02)}$ | $Q_\beta = (56 \pm 5)f^{(1.12 \pm 0.03)}$ |
| AYE | $Q_\alpha = (31 \pm 5)f^{(1.19 \pm 0.02)}$ | $Q_\beta = (72 \pm 7)f^{(1.09 \pm 0.03)}$ |
| LED | $Q_\alpha = (17 \pm 2)f^{(1.44 \pm 0.04)}$ | $Q_\beta = (67 \pm 4)f^{(1.24 \pm 0.05)}$ |
| ROT | $Q_\alpha = (25 \pm 1)f^{(1.24 \pm 0.02)}$ | $Q_\beta = (60 \pm 5)f^{(1.14 \pm 0.03)}$ |

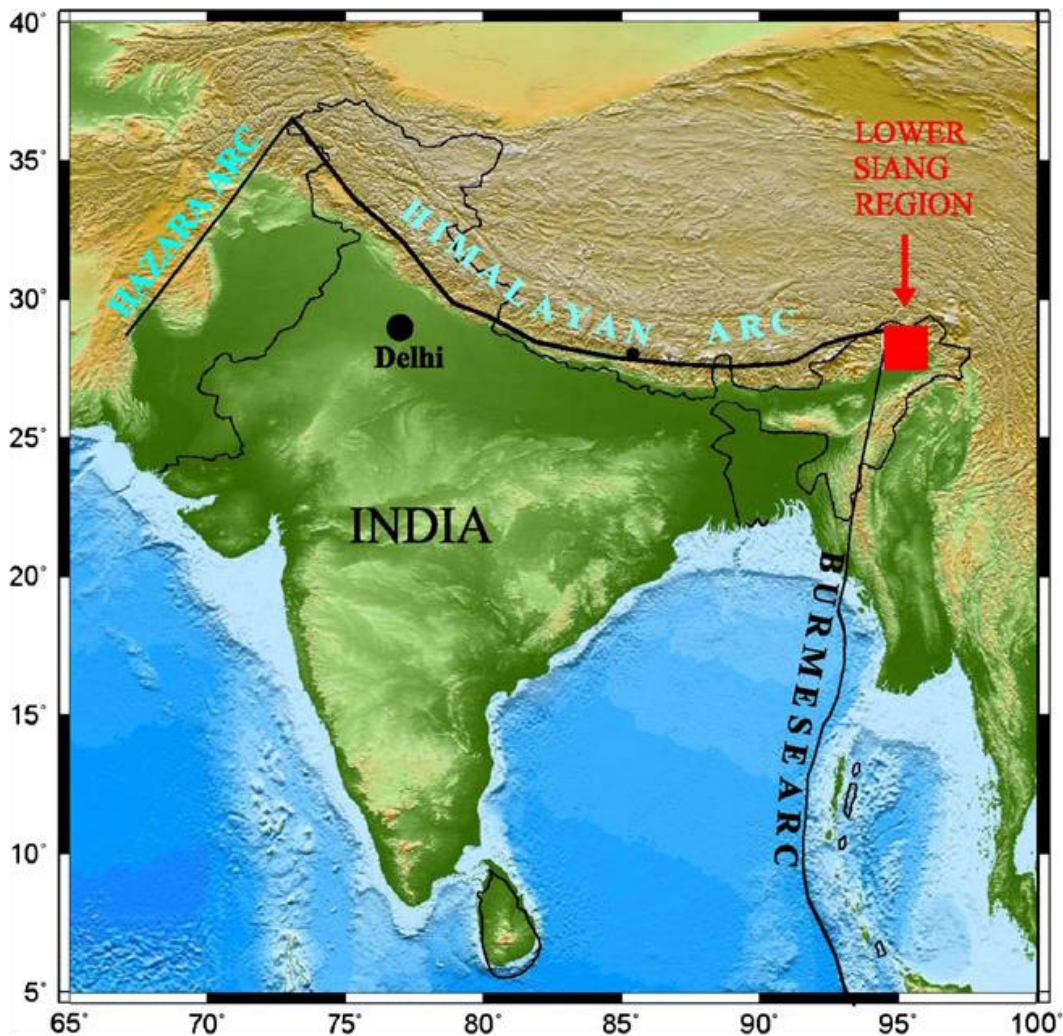


Fig. 1 Map depicts topographic map along with major tectonic fronts of the Indian Plate on north edge along the Himalaya, i.e. Hazara Arc, Himalayan Arc and Burmese Arc. The area of study is also shown as a red box in the map.

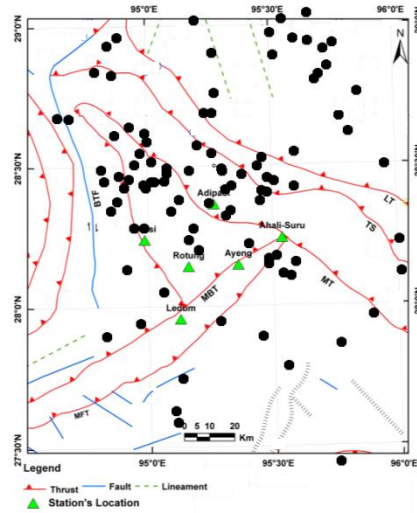


Fig 2 Map showing epicenters of events recorded during July 2011 to May 2012 (solid circles) in the Lower Siang Region. (Tectonics after GSI, 2000).

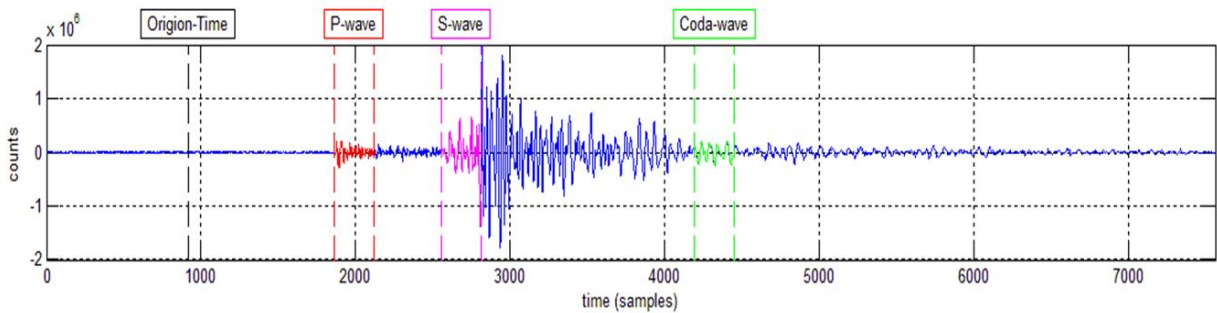
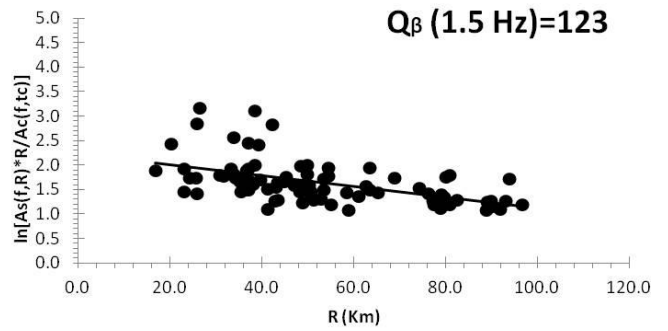
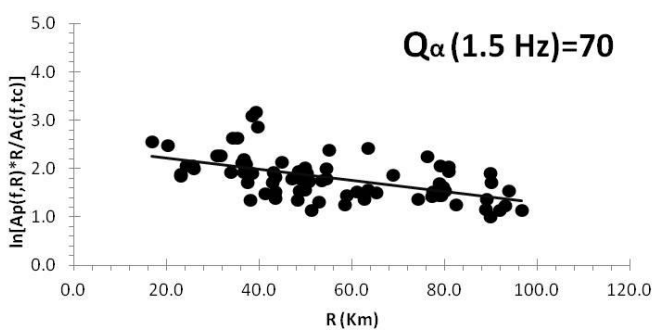
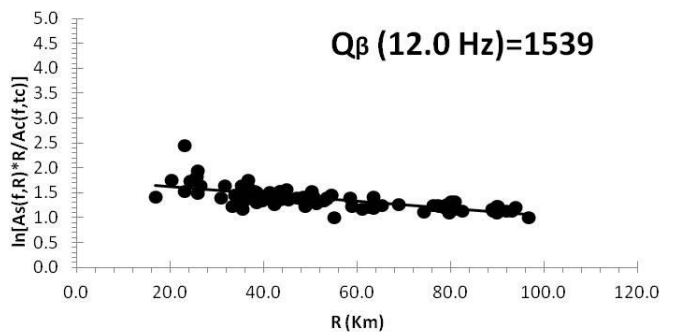
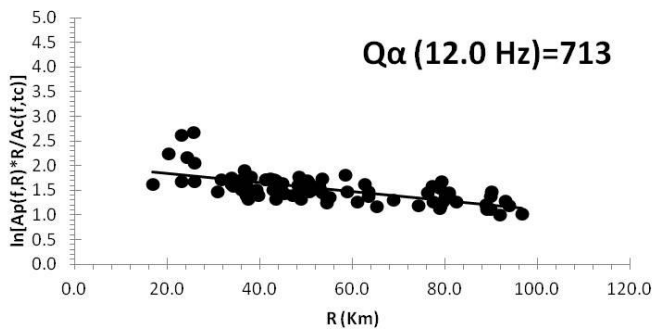
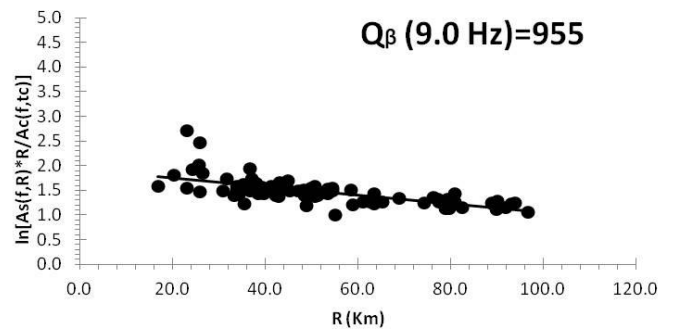
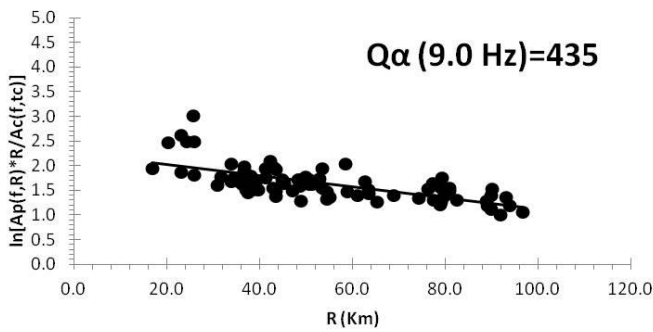
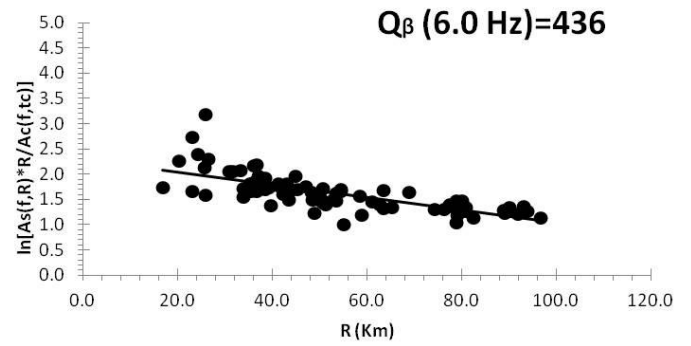
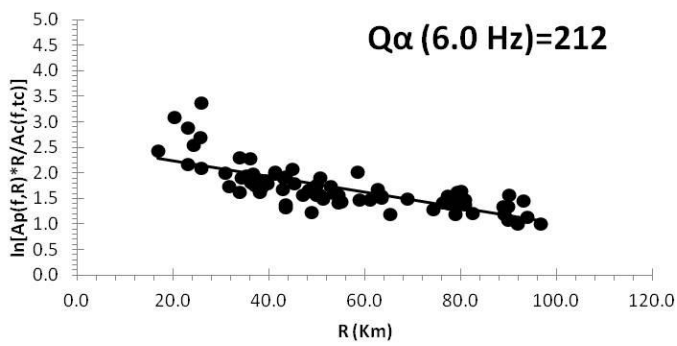
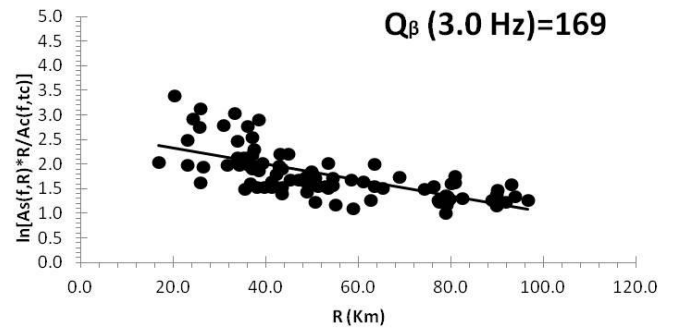
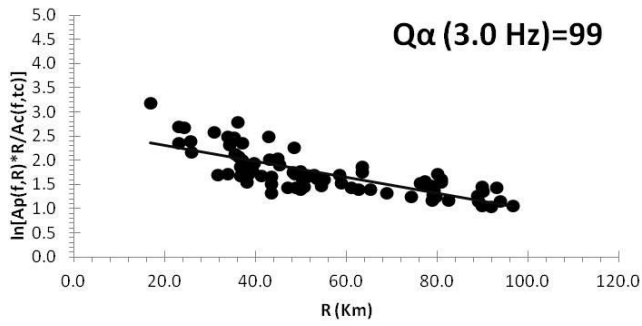


Fig 3 Example of a horizontal (N–S) component seismogram recorded at station LED with. The time of P, S and Coda waves are marked. Coda is measured for a time window of 2.56 sec with a lapse time greater than twice the travel time of S-wave.





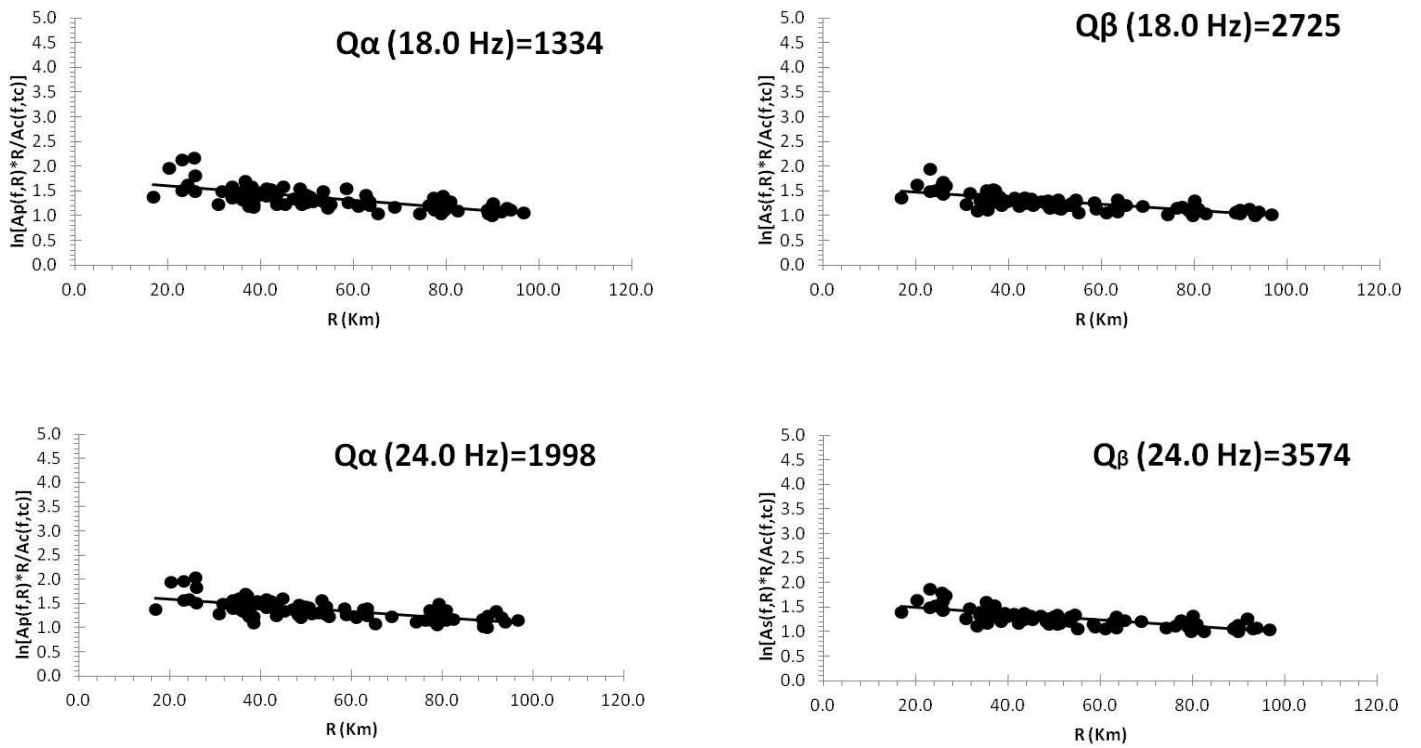


Fig 4 Coda normalized peak amplitude decay of P and S waves with hypocentral distance for five central frequencies at LED station and the regression lines from the least-squares best-fitted lines are also shown.

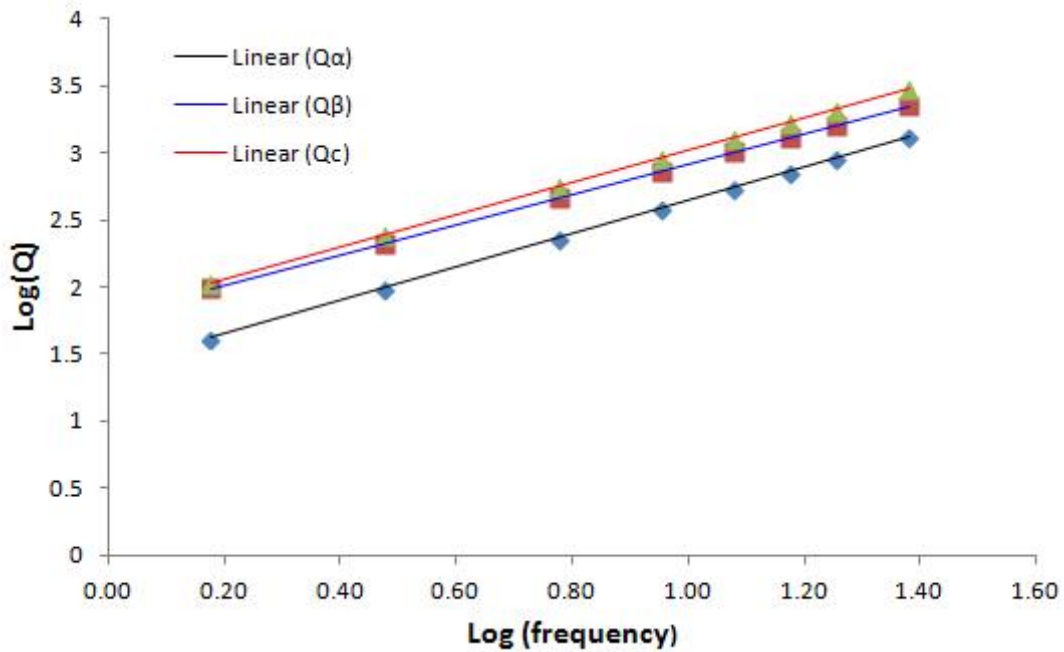


Fig 5. Average values of Q_α , Q_β , and Q_c at different frequencies for the Lower Siang region along with the least-squares best-fitted lines.

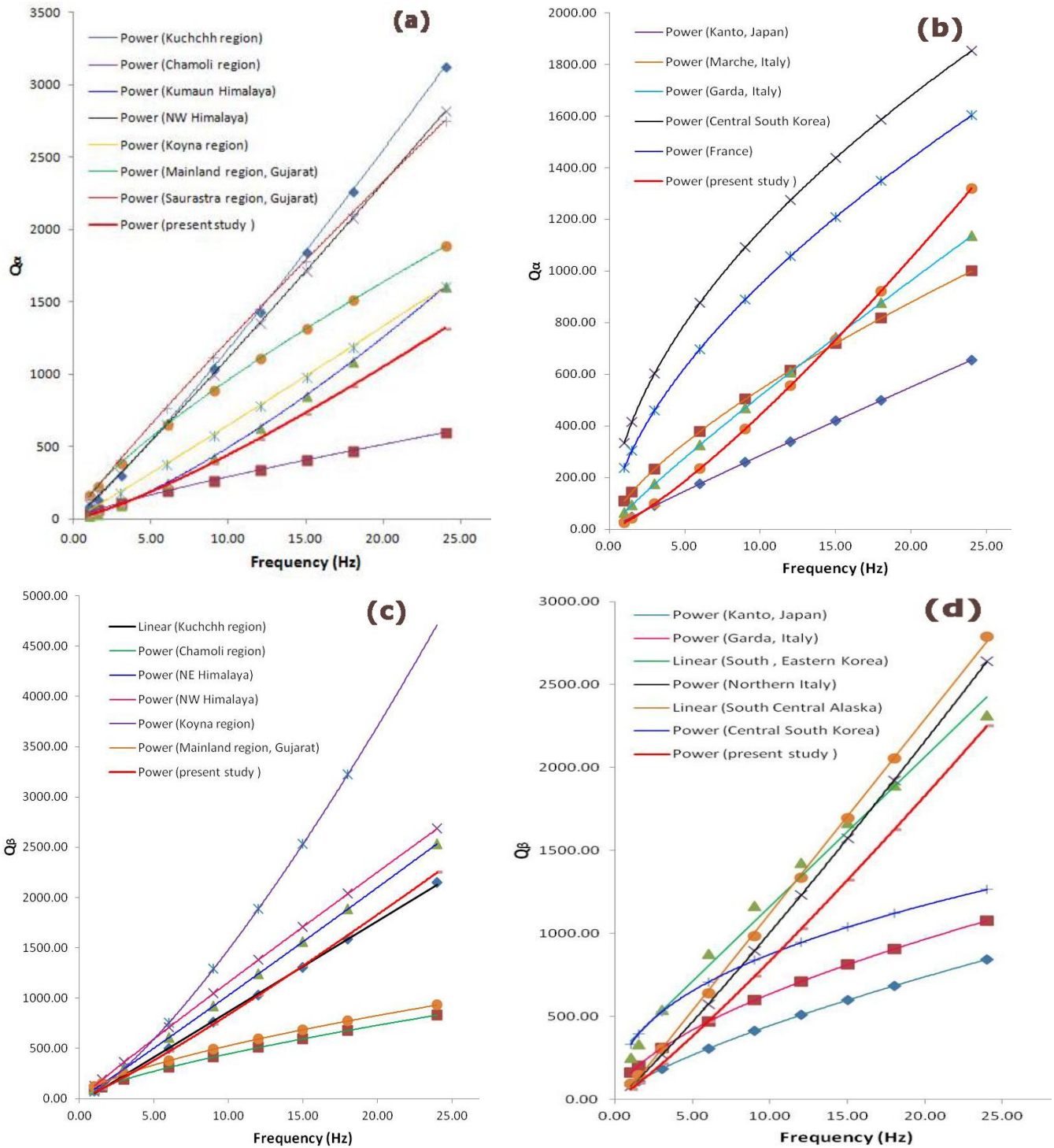


Fig 6. Comparison of Q_{α} (a,b) and Q_{β} (c, d) obtained in the present study with the other regions of the world and India such as: Kanto, Japan (Yoshimoto et al., 1993), Garda, Italy (Castro et al., 2008), South, Eastern Korea (Chung and Sato, 2001), Northern Italy (Console & Rovelli, 1981), Central Italy (Castro et al., 2002), South Central Alaska (Dutta et al., 2004), Central South Korea (Kim et al., 2004), Kuchchh region (Chopra et al., 2008), Chamoli region (Sharma et al., 2009), NE Himalaya (Padhy and Subhadra, 2010), NW Himalaya (Imtiyaz et al., 2012), Koyna region, Gujrat (Sharma, 2009), Mainland region, Gujarat (Chopra et al., 2010), Saurashtra region, Gujarat (Chopra et al., 2010), Marche, Italy (Castro, 1999), Central South Korea (Kim et al., 2004) and France (Campillo and Planet, 1991).

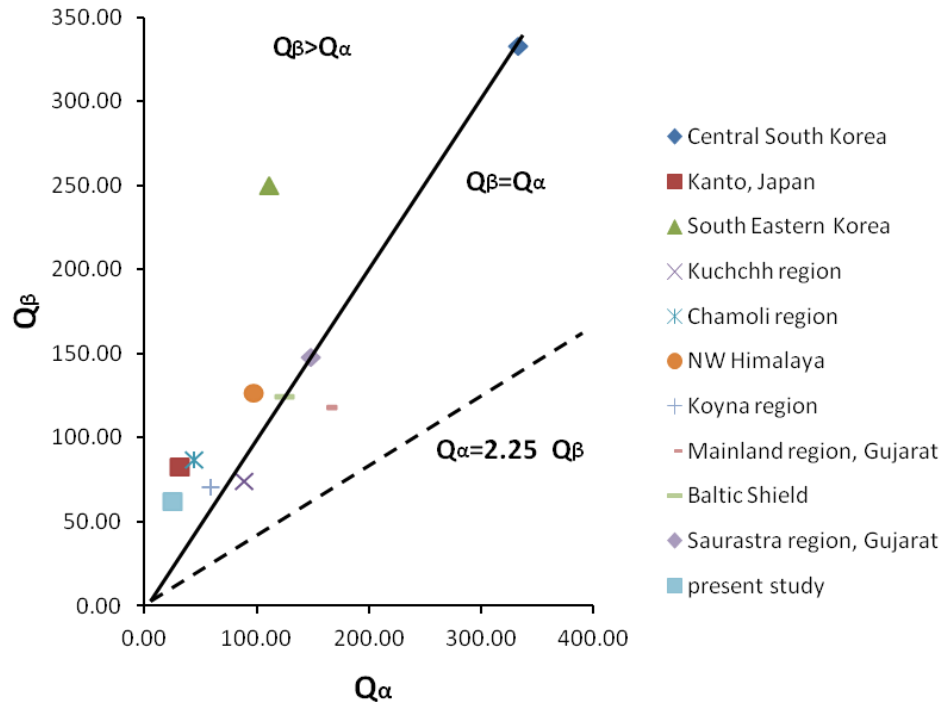


Fig 7. Comparison of average value of Q_β/Q_α (at 1 Hz) of present study with different regions of the world such as: Central South Korea (KImet et al., 2004), Kanto, Japan (Yoshimoto et al., 1993), South , Eastern Korea (Chung and Sato, 2001), Kuchchh region (Chopra et. al., 2008), Chamoli region (Sharma et al., 2009), NW Himalaya (Imtiyaz et al., 2012), Koyna region, Gujrat (Sharma, 2009), Mainland region, Gujarat (Chopra et al., 2010), Baltic Shield (Kvammeand Havskov, 1989) and Saurashtra region, Gujarat (Chopra et al., 2010). The solid line is corresponding to $Q_\beta=Q_\alpha$ and dashed line is theoretically derived by Sekiguchi (1991) corresponding to $Q_\alpha =2.25Q_\beta$.

Conclusions

For Lower Siang region of Arunachal Himalaya, the attenuation characteristics of body waves (Q_α and Q_β) have been obtained using extended coda normalization method. The obtained values of Q_α and Q_β have been found strongly frequency dependent. The frequency dependence relationships are $(25\pm 3)f^{(1.24\pm 0.04)}$ and $(62\pm 9)f^{(1.13\pm 0.04)}$ for P and S-wave respectively. The results obtained in the present study are comparable with the other seismically active regions of the world and India. The higher frequency dependence of attenuation describes the region highly seismically active. Also low value of Q_α and Q_β in the Lower Siang region indicate the high tectonic activity. The Q_α is higher than the Q_β for entire frequency range which indicate the crust of the Lower Siang region of Arunachal Himalaya is highly heterogeneous. The obtained Q_β/Q_α ratio greater than unity and the frequency dependence describe the importance of scattering attenuation. The estimated Q_β is lower than the reported Q_c value which support the Zeng et. al. (1991) model that shows Q_c contains the combined effects of intrinsic and scattering attenuation such that Q_c should be more than Q_β . Also, the obtained results are well comparable with the NE Himalaya, Kumaun Himalaya and NW Himalaya. The obtained attenuation relations in the present study will be useful for simulation of strong ground motion and for estimation earthquake source parameters which have been further required for seismic hazard assessments in this region.

ACKNOWLEDGMENTS

The authors are thankful to Prof. Ashwani Kumar, Prof. H. R. Wason, Prof. Ashok Kumar and Dr. Himanshu Mittal for their valuable guidance and support to carry out this research work. The authors are also thankful to Prof. M. L. Sharma, Head, Department of Earthquake Engineering, Indian Institute of Technology, Roorkee to provide facilities to carry out this research work and Jaypee Ventures Pvt. Ltd., Noida for funding project under which data is collected.

Reference

- Abercrombie, R.E. (1997): Near surface wave attenuation and site effects from comparison of surface and deep borehole recordings. *Bull. Seismol. Soc. Am.*, 87:731–744.
- Abdel-Fattah, A. K. (2009): Attenuation of body waves in the crust beneath the vicinity of Cairo Metropolitan area Egypt using coda normalization method. *Geophys. J. Int.*, 176:126-134.
- Aki, K., Chouet, B. (1975): Origin of the Coda waves: Source attenuation and scattering effects. *J. Geophys. Res.*, 80:3322–3342.
- Aki, K. (1980): Attenuation of shear waves in the lithosphere for frequencies from 0.05 to 25 Hz. *Phys. Earth Planet. Inter.*, 21:50–60.
- Aki, K. (1969): Analysis of seismic coda of local earthquakes as scattered waves. *J. Geophys. Res.*, 74:615–631.
- Anderson, D. L., Ben-Menahem, A., Archambeau, C. B. (1965): Attenuation of seismic energy in the upper mantle. *J. Geophys. Res.*, 70:1441-1448.
- Anderson, J. G., Lee, Y., Zeng, Y., Day, S. (1996): Control of strong motion by the upper 30 meters. *Bull. Seismol. Soc. Am.*, 86:1749–1759.
- Bianco, F., Castellano, M., Del Pezzo, E., Ibañez, J.M. (1999): Attenuation of short-period seismic waves at Mt. Vesuvius, Italy. *Geophys. J. Int.*, 138:67–76.
- Campillo, M., Plantet, J. L. (1991): Frequency dependence and spatial distribution of seismic attenuation in France: experimental results and possible interpretations. *Phys. Earth Planet. Inter.*, 67:48–64.
- Castro, R. R., Monachesi, G., Mucciarelli, M., Trojani, L., Pacor, F. (1999): P-and S-wave attenuation in the region of Marche, Italy. *Tectonophysics*, 302:123-132.
- Castro, R.R., Monachesi, M., Trojani, L., Mucciarelli, M., Frapiccini, M. (2002): An attenuation study using earthquakes from the 1997 Umbria-Marche sequence. *J. Seismol.*, 6:43–59.
- Castro, R. R., Massa, M., Augliera, P., Pacor, F. (2008): Body-wave attenuation in the region of Garda, Italy. *Pure Appl. Geophys.*, 165:1351-1366.
- Chopra, S., Kumar, D., Rao, K. M. (2008): Attenuation of P and S waves in the Kachchh Region. *J. Ind. Geophys. Union*, 121:11-22.
- Chopra, S., Kumar, D., Rastogi, B.K. (2010): Attenuation of high frequency P and S waves in the Gujarat Region, India. *Pure Appl. Geophys.*, 168:797–813.
- Chung, T.W., Sato, H. (2001): Attenuation of high-frequency P and S waves in the crust of southeastern South Korea. *Bull. Seismol. Soc. Am.*, 91:1867–1874.
- CISMHE (2011): Environmental Impact Assessment of Lower Siang H. E. Project, Arunachal Pradesh. University of Delhi.
- Console, R., Rovelli, A. (1981): Attenuation parameters for Friuli region from strong-motion accelerogram spectra. *Bull. Seismol. Soc. Am.*, 71(6).
- Der, Z.A. (1998): High frequency P and S wave attenuation in the Earth. *Pure Appl. Geophys.*, 153:273–310.
- Dutta, U., Biswas, N.N., Adams, D.A., Papageorgiou, A. (2004): Analysis of S-wave attenuation in South-Central Alaska. *Bull. Seismol. Soc. Am.*, 94:16–28.
- Fedotov, S.A., Boldyrev, S.A. (1969): Frequency dependence of the body wave absorption in the crust and the upper mantle of the Kuril Island chain. *Izv. Acad. Sci. USSR. Solid Earth*, 11:553–562.
- Gansser, A. (1964): *Geology of the Himalayas*. Interscience Publishers London. 286p.
- Gupta, S.C., Singh, V.N., Kumar, A. (1995): Attenuation of coda waves in the Garhwal Himalaya, India. *Phys. Earth Planet. Inter.*, 87:247–253.
- Gupta, S. C., Teotia, S. S., Rai, S. S., Gautam, N. (1998): Coda Q estimates in the Koyna region, India. *Pure Appl. Geophys.*, 153:713–731.
- Hermann, R. (1980): Q estimates using coda of local earthquakes. *Bull. Seismol. Soc. Am.*, 70: 447–468.
- Herrmann, R.B., Kijko, A. (1983): Modelling some empirical vertical component Lg relations. *Bull. Seismol. Soc. Am.*, 73:157–171.
- Hough, S.E., Anderson, J.G. (1988): High-frequency spectra observed at Anza, California: implications for Q structure. *Bull. Seismol. Soc. Am.*, 78:692–707.
- Khattri, K., Wyss, M., Gaur, V. K., Saha, S. N., Bansal, V. K. (1983): Local seismic activity in the region of the Assam gap, northeast India. *Bull. Seismol. Soc. Am.*, 73(2):459-469.
- Kim, K.D., Chung, T.W., Kyung, J.B. (2004): Attenuation of high-frequency P and S waves in the crust of Choongchung provinces, Central South Korea. *Bull. Seismol. Soc. Am.*, 94:1070–1078.
- Knopoff, L. (1964): *Q. Rev. Geophys.*, 2:625–660.

- Kumar, A. (2011): Study of earthquake source parameters using microearthquakes and strong motion data." Indian Institute of Technology, Roorkee.
- Kumar, A., Gupta, S. C., Kumar, A., Sen, A., Jindal, A. K., Jain, S. (2006): Estimation of source parameters from local earthquakes in Western part of the Arunachal Lesser Himalaya. In 13th Symposium on Earthquake Engineering (pp. 9-17).
- Kumar, A., Mittal, H., Sachdeva, R., Kumar, A. (2012): Indian strong motion instrumentation network. *Seismological Research Letters*, 83(1), 59-66.
- Kumar, A., Kumar, A., Gupta, S. C., Mittal, H., Kumar, R. (2013a): Source parameters and f_{max} in Kameng region of Arunachal Lesser Himalaya. *Journal of Asian Earth Sciences*, 70(71):35-44.
- Kumar, R., Gupta, S. C., Kumar, A., Mittal, H. (2013b). Source parameters and f_{max} in lower Siang region of Arunachal lesser Himalaya. *Arabian Journal of Geosciences*, 1-11.
- Kumar, G. (1997): *Geology of Arunachal Pradesh*. Geological Society of India, Bangalore, pp.1-217.
- Kumar, R., Gupta, S.C., Kumar, A. (2014): Coda wave attenuation characteristics for Lower Siang region of Arunachal Himalaya. *Tectonophysics*, (under review).
- Kvamme, L.B., Havskov, J. (1989): Q in Southern Norway. *Bull. Seismol. Soc. Am.*, 79:1575–1588.
- Liu, H. P., Anderson, D. L., Kanamori, H. (1976): Velocity Dispersion due to Anelasticity; Implications for Seismology and Mantle Composition. *Geophys. J. R. Astr. Soc.*, 47:41–58.
- Ma'hood, M., Hamzehloo, H., Doloei, G.J., 2009. Attenuation of high frequency P and S waves in the crust of the East-Central Iran. *Geophys. J. Int.* 179, 1669–1678
- Mandal, P., Padhy, S., Rastogi, B.K, Satyanarayana, H.V.S., Kousalaya M., Vijayraghavan, R., Srinivasan, A. (2001): Aftershock activity and frequency-dependent low coda Q_c in the epicentral region of the 1999 Chamoli earthquake of magnitude Mw 6.4. *Pure. Appl. Geophys.*, 158:1719–1735.
- Mandal, P., Jainendra S. J, Sudesh, K. Rajender, B., Rastogi, B. K. (2004): Low coda Q_c in the epicentral region of 2001 Bhuj Earthquake of Mw 7.7. *Pure Appl. Geophys.*, 161:1635–1654.
- Masuda, T. (1988): Corner frequencies and Q values of P waves by simultaneous inversion technique. *Sci. Rep. to Univ. Ser. 5. Geophys.*, 31:101–125.
- Mayeda, K., Hofstetter, A., O'Boyle, J. L., Walter, W. R. (2003): Stable and transportable regional magnitudes based on coda-derived moment-rate spectra. *Bull. Seismol. Soc. Am.*, 93:224-239.
- Mitchell, B. J. (1995): Anelastic structure and evolution of the continental crust and upper mantle from seismic surface wave attenuation. *Reviews of Geophysics*, 33:441-462.
- Molnar, P., Tucker, B. E., Brune, J. N. (1973): Corner frequencies of P and S waves and models of earthquake sources. *Bull. Seismol. Soc. Am.*, 63(6-1):2091-2104.
- Molnar, P. (1990): A review of the seismicity and the rates of active under thrusting and deformation at the Himalaya. *Jr. Him. Geol.*, 2:131–154.
- Narula, P.L., Shanker, R., Chopra, S. (2000): Rupture mechanism of Chamoli earthquake on 29 March 1999 and its implication for seismotectonics of Garhwal Himayala. *J. Geol. Soc. of India*, 55:493-503.
- Ni, J., Barazangi, M. (1984): Seismotectonics of the Himalayan collision zone: Geometry of the underthrusting Indian plate beneath the Himalaya. *J. Geophys. Res.*, 89:1147–1163.
- Padhy, S. (2009): Characteristics of body wave attenuations in the Bhuj crust. *Bull. Seismol. Soc. Am.*, 99:3300–3313.
- Paul, A., Gupta, S. C., Pant, C. C. (2003): CODA Q estimates for Kumaun Himalaya. *J. Earth System Science*, 112(4):569-576.
- Padhy, S., Subhadra, N. (2010): Attenuation of high-frequency seismic waves in northeast India. *Geophys. J. Int.*, 181:453–467.
- Parvez, I. A., Yadav, P., Nagaraj, K. (2012): Attenuation of P, S and Coda Waves in the NW-Himalayas, India. *Int. J. Geosciences*, 3(1).
- Rautian, T.G., Khalturin, V.I. (1978): The use of the coda for the determination of the earthquake source spectrum. *Bull. Seismol. Soc. Am.*, 68:923–948.
- Rautian, T.G., Khalturin, V.I., Martynov, V.G., Molnar, P. (1978): Preliminary analysis of the spectral content of P and S waves from local earthquakes in the Garm, Tadjikistan region. *Bull. Seismol. Soc. Am.*, 68:949–971.
- Sato, H. (1992): Thermal Structure of the Mantle Wedge beneath Northeastern Japan: Magmatism in an Island Arc from the Combined Data of Seismic Anelasticity and Velocity and Heat Flow. *J. Volcanol. Geotherm. Res.*, 51:237–252.
- Sato, H., Fehler, M.C. (1998): *Seismic Wave Propagation and Scattering in the Heterogeneous Earth*. Springer-Verlag, New York, pp. 308.

- Sekiguchi, S. (1991): Three-dimensional Q structure beneath Kanto-Tokai district, Japan. *Tectonophysics*, 195:83–104.
- Sharma, B., Teotia, S.S., Kumar, D. (2007): Attenuation of P, S and coda waves in Koyna region, India. *J. Seismol.*, 11:327–344.
- Sharma, B., Gupta, A. K., Devi, D. K., Kumar, D., Teotia, S. S., Rastogi, B. K. (2008): Attenuation of high-frequency seismic waves in Kachchh Region, Gujarat, India. *Bull. Seismol. Soc. Am.*, 985:2325-2340.
- Sharma, B., Teotia, S. S., Kumar, D., Raju, P. S. (2009): Attenuation of P-and S-waves in the Chamoli Region, Himalaya, India. *Pure and applied geophysics*, 166(12):1949-1966.
- Singh, C., Singh, A., Bharathi, V. K., Bansal, A. R., Chadha, R. K. (2012): Frequency-dependent body wave attenuation characteristics in the Kumaun Himalaya. *Tectonophysics*, 524:37-42.
- Singh, I. B. (1996): Geological evolution of Ganga Plain – an overview. *J. Palaeont. Soc. India*, 41:99–137.
- Singh, S. (1993): Geology and tectonics of the Eastern Syntaxial Bend, Arunachal Himalaya. *Jour. Himalayan Geol.*, 2:149-163.
- Toksoz, M.N., Johnston, A.H., Timur, A. (1978): Attenuation of seismic waves in dry and saturated rocks. I. Laboratory measurements. *Geophys.*, 44:681–690.
- Wennerberg, L. (1993): Multiple-scattering interpretations of coda-Q measurements. *Bull. Seismol. Soc. Am.*, 83:279–290.
- Yoshimoto, K., Sato, H., Ohtake, M. (1993): Frequency-dependent attenuation of P and S waves in the Kanto area, Japan, based on the coda normalization method. *Geophys. J. Int.*, 114:165–174.
- Yoshimoto, K., Sato, H., Ito, Y., Ito, H., Ohminato, T., Ohtake, M. (1998): Frequency-dependent attenuation of high-frequency P and S waves in the upper crust in western Nagano, Japan. *Pure Appl. Geophys.*, 153:489–502.
- Zeng, Y., Su, F., Aki, K. (1991): Scattered wave energy propagation in a random isotropic scattering medium, I, theory. *J. Geophys. Res.*, 96:607–619.